Electron-impact excitation cross sections of vibrationally excited $X\,^1\Sigma_g^+$ H_2 and D_2 molecules to Rydberg states

R. Celiberto,[1,2] A. Laricchiuta,[3] U. T. Lamanna,[3,4] R. K. Janev,[5] and M. Capitelli[2,3]
[1]*Politecnico di Bari, Bari, Italy*
[2]*Centro di Studio per la Chimica dei Plasmi del CNR, Bari, Italy*
[3]*Dipartimento di Chimica, Università di Bari, Italy*
[4]*Centro Studi Chimico-Fisici sull'Interazione Luce Materia, Bari, Italy*
[5]*International Atomic Energy Agency, Vienna, Austria*
(Received 23 December 1998)

A complete set of total and dissociative electron-impact cross sections of vibrationally excited H_2 and D_2 molecules has been calculated by using the impact-parameter method. Transitions to low-lying Rydberg states ($X\rightarrow B', X\rightarrow B'', X\rightarrow D, X\rightarrow D'$) are considered. Finally, vibrational and mass scaling relations, able to reproduce the calculated cross sections, are presented. [S1050-2947(99)00609-5]

PACS number(s): 34.60.+z, 34.80.Gs, 52.20.Fs

I. INTRODUCTION

Dissociative attachment from vibrationally excited H_2 and D_2 molecules, in their ground electronic state, is the main accepted mechanism for the H^- and D^- negative-ion production in multicusp magnetic plasma [1,2]. Cross sections and rate coefficients for this process have been well established [3] and their main feature is the dramatic enhancement that they undergo as the vibrational state of the molecule is increased.

Recently [4,5] an efficient H^- formation channel involving dissociative attachment from electronically excited molecules has been reported. This process can be described as

$$H_2^* + e \rightarrow H + H^-, \tag{1.1}$$

where H_2^* represents a hydrogen molecule in a high-lying excited Rydberg state. This result pushed some authors to investigate the role of excited electronic states in H^- formation kinetics [6–9].

A general feature shown by these calculations is the need for more reliable input data, concerning, in particular, the electron-molecule cross sections for electronic transitions, the knowledge of which is limited to a few low-lying Rydberg states and practically referred only to molecules initially in their ground vibrational state.

Divertor plasmas provide a further example of a plasma system where a non-negligible concentration of molecular electronically excited states might be present. These devices, studied in nuclear fusion, are important components of the next generation fusion reactors [10]. The relatively low temperatures achieved in the external region ($T_e \sim 1-10$ eV) allow for the formation of atomic and molecular hydrogen, in the ground and excited states.

Thereby, the knowledge of electron-molecule cross sections for processes involving Rydberg states becomes essential for an accurate description of hydrogen plasmas. Collisional-radiative models, for instance, have been developed for divertor and edge plasmas [11–14] as well as for hydrogen discharges [6–9]. Excitation from the ground electronic state to a wide spectrum of Rydberg states has been considered, and the cross sections for these processes have been evaluated by resorting to approximated scaling laws expressed in terms of the atomic principal quantum number ($\sigma \propto n^{-3}$) [6,14,15].

In this paper we present a complete set of cross sections, as a function of incident energy and vibrational quantum number for both the H_2 and D_2 molecules, for the process

$$M_2(X\,^1\Sigma_g^+, \nu_i) + e \rightarrow M_2^* + e, \tag{1.2}$$

where M_2 stands either for the H_2 or D_2 isotope, $X\,^1\Sigma_g^+$ is the ground electronic state, and M_2^* represents an electronically excited molecule. We consider the excitation to the following molecular states: $B'\,^1\Sigma_u^+(3p\sigma)$, $D\,^1\Pi_u(3p\pi)$, $B''\,^1\Sigma_u^+(4p\sigma)$, $D'\,^1\Pi_u(4p\pi)$, where the symbol in parentheses is the usual state notation in the united-atom limit [16]. The cross sections for the process (1.2) have been evaluated by using the impact-parameter method, while the transition dipole moments, required by the method, were obtained by performing full configuration interaction calculations.

A brief account of the method and numerical details are given in Secs. II and III, respectively. Results are discussed in Sec. IV and some analytical expressions to fit the calculated cross sections are presented in Sec. V. Finally, some comments and conclusions are given in Sec. VI.

II. METHOD OF CALCULATION

We collect in this section the relevant equations of the impact-parameter method. The formulation of the method and its applications to electron-molecule scattering can be found elsewhere [17–22].

The *total cross section* (excitation plus dissociative excitation) for a vibroelectronic excitation of a molecule from the α_i to the α_f electronic state, induced by electron impact at an incident energy E, is given by

$$\sigma_{\nu_i}^{\alpha_i\rightarrow\alpha_f}(E) = \sum_{\nu_f} \sigma_{\nu_i,\nu_f}^{\alpha_i\rightarrow\alpha_f}(E) + \int_{\epsilon_{\min}}^{\epsilon_{\max}} d\epsilon \frac{d\sigma_{\nu_i,\epsilon}^{\alpha_i\rightarrow\alpha_f}(E)}{d\epsilon}, \tag{2.1}$$

where ν_i and ν_f are the initial and final vibrational quantum numbers, respectively. The sum on the first term on the right hand side includes all the bound vibrational levels of the α_f electronic state, while the integration on the second term is extended to the continuum vibrational spectrum of the α_f state, with ϵ ranging between the dissociation threshold $\epsilon_{\min}$ and upper limit $\epsilon_{\max}$ defined as

$$\epsilon_{\max}=E+\epsilon_{\nu_i}^{\alpha_i}, \tag{2.2}$$

where ϵ_ν^α indicates the energy eigenvalue of the νth vibrational level belonging to the α electronic state. The two terms in Eq. (2.1) give, respectively, the contributions coming from the *excitation* (bound-bound) and *dissociative excitation* (bound-continuum) to the total cross section.

The expression for $\sigma_{\nu_i,\nu_f}^{\alpha_i\to\alpha_f}(E)$ in the impact-parameter method is written as

$$\sigma_{\nu_i,\nu_f}^{\alpha_i\to\alpha_f}(E)=S_{\nu_i,\nu_f}^{\alpha_i,\alpha_f}D_{\nu_i,\nu_f}^{\alpha_i,\alpha_f}(E), \tag{2.3}$$

where the ''structural factor'' is defined by

$$S_{\nu_i,\nu_f}^{\alpha_i,\alpha_f}=\frac{m^2e^2}{3g_i\hbar^4}(2-\delta_{\Lambda_i,0})(2-\delta_{\Lambda_f,0})\times\left|\int_0^\infty dR\chi_{\nu_f}^{\alpha_f}(R)M_{\Lambda_i,\Lambda_f}^{\alpha_i,\alpha_f}(R)\chi_{\nu_i}^{\alpha_i}(R)\right|^2. \tag{2.4}$$

In this expression $m,e,\hbar$, and g_i represent, in order, mass and charge of electron, Planck's constant, and a degeneracy factor for the α_i state. $\chi_\nu^\alpha(R)$ is the vibrational wave function depending on the internuclear distance R, and $M_{\Lambda_i,\Lambda_f}^{\alpha_i,\alpha_f}(R)$ is the usual electronic transition dipole moment characterized by the quantum numbers of the projection of the electronic angular momentum on the internuclear axis Λ_i and Λ_f.

The ''dynamical factor'' is given by

$$\begin{aligned}D_{\nu_i,\nu_f}^{\alpha_i,\alpha_f}=\frac{2\pi\hbar^2}{m^2u_i^2}\Bigg\{&\gamma_i\left(K_0(\gamma_i)K_1(\gamma_i)-\frac{\pi^2}{4}S_0(\gamma_i)S_1(\gamma_i)\right)+\gamma_f\left(K_0(\gamma_f)K_1(\gamma_f)-\frac{\pi^2}{4}S_0(\gamma_f)S_1(\gamma_f)\right)\\&+\gamma\left(K_0(\gamma_i)K_1(\gamma_f)+K_0(\gamma_f)K_1(\gamma_i)+\frac{\pi^2}{4}S_0(\gamma_i)S_1(\gamma_f)+\frac{\pi^2}{4}S_0(\gamma_f)S_1(\gamma_i)\right)\\&+\left(\frac{u_i^2-u_f^2}{u_i^2+u_f^2}\right)\left[\ln\left(\frac{\gamma_f}{\gamma_i}\right)+\frac{\pi}{2}\int_{\gamma_i}^{\gamma_f}S_0(\gamma)d\gamma\right]\Bigg\},\end{aligned} \tag{2.5}$$

where K_i and S_i are the modified Bessel functions and modified Struve functions, respectively, and u_i and u_f are the initial and final electron velocities. Moreover,

$$\gamma_i=\frac{\rho_{\nu_i,\nu_f}^0|\Delta E_{\nu_i,\nu_f}^{\alpha_i,\alpha_f}|}{\hbar}\frac{1}{u_i}, \tag{2.6}$$

$$\gamma_f=\frac{\rho_{\nu_i,\nu_f}^0|\Delta E_{\nu_i,\nu_f}^{\alpha_i,\alpha_f}|}{\hbar}\frac{u_i}{u_f^2}, \tag{2.7}$$

$$\gamma=\frac{\rho_{\nu_i,\nu_f}^0|\Delta E_{\nu_i,\nu_f}^{\alpha_i,\alpha_f}|}{\hbar}\frac{2u_i}{u_i^2+u_f^2}, \tag{2.8}$$

where $\Delta E_{\nu_i,\nu_f}^{\alpha_i,\alpha_f}$ is the transition energy defined as

$$\Delta E_{\nu_i,\nu_f}^{\alpha_i,\alpha_f}=\epsilon_{\nu_f}^{\alpha_f}-\epsilon_{\nu_i}^{\alpha_i}. \tag{2.9}$$

ρ_{ν_i,ν_f}^0 is a cutoff parameter introduced in the impact-parameter method to avoid divergent cross sections [17–19].

The dissociative cross section is defined as

$$\int d\epsilon\frac{d\sigma_{\nu_i,\epsilon}^{\alpha_i\to\alpha_f}(E)}{d\epsilon}=\int_{\epsilon_{\min}}^{\epsilon_{\max}}d\epsilon S_{\nu_i,\epsilon}^{\alpha_i,\alpha_f}D_{\nu_i,\epsilon}^{\alpha_i,\alpha_f}(E), \tag{2.10}$$

where the structural and the dynamical factors have the same expression given by Eqs. (2.4) and (2.5) provided that the discrete variable ν_f is formally replaced by the continuum energy ϵ.

The impact-parameter method, in the present formulation [18], does not include exchange effects and it is suitable for the treatment of dipole-allowed and spin-conserving excitations. At high incident energies the accuracy of the method is comparable to the Born approximation and shows good agreement with other more sophisticated methods, also in the region of intermediate energies. Resonant effects, however, which affect the cross section near the threshold, are not accounted for by the method, so that the low-energy results should be considered from a qualitative point of view. Nevertheless, useful information concerning the cross section dependence on the vibrational state of the molecule can still be obtained from the impact-parameter method, also near the energy threshold region, where reliable data, obtained with more sophisticated theories or from measurements, are at present not yet available.

III. COMPUTATIONAL DETAILS

The electronic transition dipole moments, required in the evaluation of the structural factor [Eq. (2.4)], have been calculated by performing full configuration interaction calculations by using the Slater-type orbital (STO) basis sets dis-

TABLE I. Electronic transition dipole moments (a.u.) as a function of the internuclear distance R (a.u.).

R	$X\rightarrow B'$	$X\rightarrow B''$	$X\rightarrow D$	$X\rightarrow D'$
0.5	0.2639	0.1733	0.2628	0.1807
0.7	0.2965	0.1923	0.2868	0.1956
1.0	0.3497	0.2241	0.3214	0.2164
1.2	0.3719	0.2342	0.3384	0.2259
1.4	0.4021	0.2492	0.3573	0.2360
1.5	0.4155	0.2551	0.3659	0.2404
1.6	0.4274	0.2597	0.3739	0.2442
1.7	0.4377	0.2630	0.3813	0.2474
1.8	0.4460	0.2647	0.3880	0.2502
1.9	0.4521	0.2647	0.3940	0.2524
2.0	0.4314	0.2388	0.3900	0.2505
2.2	0.4215	0.2232	0.4008	0.2544
2.5	0.3860	0.1886	0.4120	0.2558
3.0	0.2790	0.1064	0.4175	0.2486
3.5	0.1251	0.0045	0.4378	0.2591
4.0	0.0587	0.1274	0.4391	0.2594
4.5	0.2301	0.2169	0.4421	0.2654
5.0	0.3574	0.2561	0.4473	0.2789
5.5	0.4424	0.2666	0.4520	0.3012
6.0	0.4987	0.2321	0.4541	0.2267
6.5	0.5373	0.6432	0.4537	0.1175
7.0	0.5646	0.7074	0.4522	0.0713
7.5	0.5843	0.7462	0.4509	0.0537
8.0	0.5986	0.7666	0.4502	0.0516
8.5	0.6095	0.7739	0.4499	0.0573
9.0	0.6187	0.7713	0.4501	0.0664
9.5	0.6289	0.7599	0.4505	0.0765
10.0	0.6440	0.7395	0.4513	0.0865

cussed in Ref. [23]. The calculated values are reported in Table I. These results have been checked in the range $1 \leqslant R \leqslant 3$ a.u. by comparison with those obtained by Branchett and Tennyson [24]. In general we have found a satisfactory agreement, the differences not exceeding 20%. For the $X \rightarrow B'$ and $X\rightarrow D$ transitions at $R=1$ a.u., the results of Ref. [24] seem particularly low (~ 0.22 and ~ 0.27 a.u., respectively). However, our value of 0.3497 a.u. for the $X\rightarrow B'$ is in better agreement with the results reported by Ford *et al.* [25] (0.3306 a.u.) and Borges *et al.* [26] (0.3262 a.u.) at the same internuclear distance.

The potential energies used to obtain the vibrational wave functions and eigenvalues for the $X\,^1\Sigma_g^+$, $B'\,^1\Sigma_u^+$, $B''\,^1\Sigma_u^+$, and $D\,^1\Pi_u$ electronic states have been taken from the literature [27–29] except for a few points needed for short range extrapolations (Table II). For the $D'\,^1\Pi_u$ state the potential energies have been obtained by configuration interaction calculations by using the same basis set cited above [23]. The numerical values for this state are given in Table II. These energies have been used for both the H_2 and D_2 molecules.

The structural factor has been calculated by performing a Gaussian quadrature for the integration in Eq. (2.4), linearly interpolating the dipole moments from the data of Table I in the required integration points. The bound vibrational wave functions entering in the integrand have been computed solving the radial Schrödinger equation by expanding the function χ_ν^α in terms of harmonic oscillators for all the electronic states but the $B''\,^1\Sigma_u^+$. In this last case, since the expansion showed a very low convergence due to the presence of the double minimum in the potential curve, we have used the algorithm developed by Tobin and Hinze [30].

The potential curves entering in the vibrational Schrödinger equation, have been extrapolated in the asymptotic regions. In particular, for short internuclear distances we assumed for the potential function the following form [22]:

$$V_\alpha(R)=A\frac{e^{-BR}}{R}, \tag{3.1}$$

where the constants A and B were obtained for each electronic state by fitting the first two points of Table II. In the region of long range forces, the potential curves have been extrapolated in the usual form as [18,22]

$$V_\alpha(R)=V_\alpha^\circ(R)-\frac{C_6}{R^6}-\frac{C_8}{R^8} \tag{3.2}$$

utilizing the last two points at largest available internuclear distances (see Refs. [27–29] and Table II).

The continuum vibrational wave functions required for dissociative cross sections have been computed by using the method illustrated in Ref. [21]. The integral in Eq. (2.10) on the continuum energy has been evaluated by using the Simpson rule, stopping the integration to a suitable value of the variable $\epsilon(<\epsilon_{\max})$, beyond which the integrand can be assumed negligible.

The evaluation of the ''dynamical factor'' requires the transition energy, defined in Eq. (2.9), and the cutoff parameter $\rho^0_{\nu_i,\nu_f}$, which has been adjusted to a suitable value by imposing that the impact-parameter method reproduces at high incident energies the Born-approximation total cross sections [22]. With this definition the cutoff parameter no longer depends on the final vibrational quantum number ν_f.

IV. RESULTS

Figures 1(a)–1(d) show the total e-H_2 cross sections for the four transitions considered here, as a function of the incident energy. Each curve refers to a given value of the initial vibrational quantum number ν_i which ranges in the interval 0–14.

The cross section maximum for the $X\rightarrow B'$ transition [Fig. 1(a)] shows a regular enhancement up to $\nu_i=9$ (solid lines), then rapidly decreases for higher ν_i (dashed lines). This ν_i dependence has been observed also for the $X\,^1\Sigma_g^+ \rightarrow B\,^1\Sigma_u^+(2p\sigma)$ transition [20] for which it has been shown that it is mainly due to the behavior of the dipole moment as a function of the internuclear distance. The total cross sections for the $X\rightarrow B''$ transition [Fig. 1(b)] display smaller values with respect to the previous case and more irregular behavior in terms of the vibrational quantum number.

The two following $^1\Sigma\rightarrow{}^1\Pi$ excitations, $X\rightarrow D$ [Fig. 1(c)] and $X\rightarrow D'$ [Fig. 1(d)], show similar dependence on ν_i. In both cases, in fact, the cross section monotonically increases up to $\nu_i=13$, while its maximum value undergoes an enhancement about a factor of 1.5 passing from $\nu_i=0$ to ν_i

TABLE II. Potential energies (hartrees) as a function of the internuclear distance R (a.u.) for B', B'', D, D' electronic states.

R	$B'\,^1\Sigma_u^+$	$B''\,^1\Sigma_u^+$	$D\,^1\Pi_u$	$D'\,^1\Pi_u$	R	$B'\,^1\Sigma_u^+$	$B''\,^1\Sigma_u^+$	$D\,^1\Pi_u$	$D'\,^1\Pi_u$
0.500	0.2112	0.2356	0.2124	0.2364	4.250	−0.6292	−0.5849		
0.700	−0.2369	−0.2124	−0.2350	−0.2112	4.500	−0.6278	−0.5812	−0.5853	−0.5612
1.000	−0.5086	−0.4825	−0.5060	−0.4808	4.750	−0.6270	−0.5775		
1.100	−0.5536	−0.5280	−0.5505		5.000	−0.6266	−0.5741	−0.5762	−0.5521
1.200	−0.5866	−0.5610	−0.5829	−0.5580	5.250	−0.6264	−0.5710		
1.250	−0.5997		−0.5956		5.500	−0.6263	−0.5685	−0.5696	−0.5457
1.300	−0.6109		−0.6065		5.750	−0.6263	−0.5680		
1.400	−0.6287	−0.5986	−0.6236	−0.5988	6.000	−0.6263	−0.5709	−0.5650	−0.5437
1.500	−0.6416		−0.6358		6.500	−0.6262	−0.5767	−0.5618	−0.5447
1.600	−0.6509	−0.6240	−0.6442	−0.6193	7.000	−0.6261	−0.5829	−0.5597	−0.5454
1.700	−0.6573	−0.6300	−0.6498	−0.6248	7.500	−0.6260	−0.5881	−0.5583	−0.5457
1.800	−0.6616	−0.6339	−0.6532	−0.6280	8.000	−0.6259	−0.5927	−0.5574	−0.5457
1.900	−0.6642	−0.6360	−0.6549	−0.6295	8.500	−0.6258	−0.5965	−0.5568	−0.5455
1.950		−0.6364			8.750			−0.5566	
1.952			−0.6553		9.000	−0.6257	−0.5997	−0.5564	−0.5452
1.983			−0.6553		9.250			−0.5563	
2.000	−0.6655	−0.6369	−0.6553	−0.6308	9.500		−0.6022	−0.5562	−0.5448
2.020		−0.6369			10.000	−0.6255	−0.6039	−0.5560	−0.5444
2.025		−0.6369			10.500		−0.6051	−0.5559	
2.030		−0.6369			11.000	−0.6254	−0.6055	−0.5558	
2.050		−0.6369			11.250		−0.6055		
2.085	−0.6658				11.500		−0.6054		
2.100	−0.6657	−0.6367	−0.6547		12.000	−0.6253	−0.6046	−0.5557	
2.200	−0.6653	−0.6358	−0.6533	−0.6285	12.500		−0.6034		
2.300	−0.6643	−0.6342	−0.6512		13.000	−0.6252	−0.6019		
2.400	−0.6628	−0.6322	−0.6487		14.000	−0.6251	−0.5982	−0.5557	
2.430	−0.6623				15.000	−0.6251	−0.5943		
2.500	−0.6609		−0.6459	−0.6209	16.000	−0.6250		−0.5556	
2.600	−0.6589	−0.6272			17.000	−0.6250			
2.700	−0.6566				18.000	−0.6250			
2.750			−0.6378		19.000	−0.6250			
2.800	−0.6543	−0.6216			20.000	−0.6250		−0.5556	
2.900	−0.6519				21.000	−0.6250			
3.000	−0.6495	−0.6156	−0.6291	−0.6042	22.000	−0.6250			
3.250	−0.6437	−0.6083	−0.6204		23.000	−0.6250			
3.500	−0.6386	−0.6015	−0.6121	−0.5878	25.000	−0.6250		−0.5556	
3.750	−0.6345	−0.5954	−0.6044		30.000	−0.6250			
4.000	−0.6313	−0.5896	−0.5973	−0.5731					

$=13$. The $X \rightarrow D'$ transition presents, however, smaller cross sections. The total cross sections, as well as the dissociative ones discussed below, present in some cases a sharp peak, also observed in other situations [19,20,22], located very close to the threshold energy. This feature seems to artificially introduce some resonant effects in the impact-parameter method at low incident energies [31].

Figures 2(a)–2(d) show the total cross sections for the corresponding transitions in the D_2 molecule. Their behavior in terms of vibrational quantum number, which lies now in the range 0–20, is quite similar to the one just discussed for the H_2 case.

Dissociative cross sections are displayed in Figs. 3(a)–3(d) and 4(a)–4(d) for H_2 and D_2, respectively. Their dependence on ν_i can be better appreciated in Fig. 5(a)–5(d) where the total and dissociative cross sections, for both the isotopes, are plotted as a function of the initial vibrational quantum number and for a fixed incident energy of 42 eV. For the

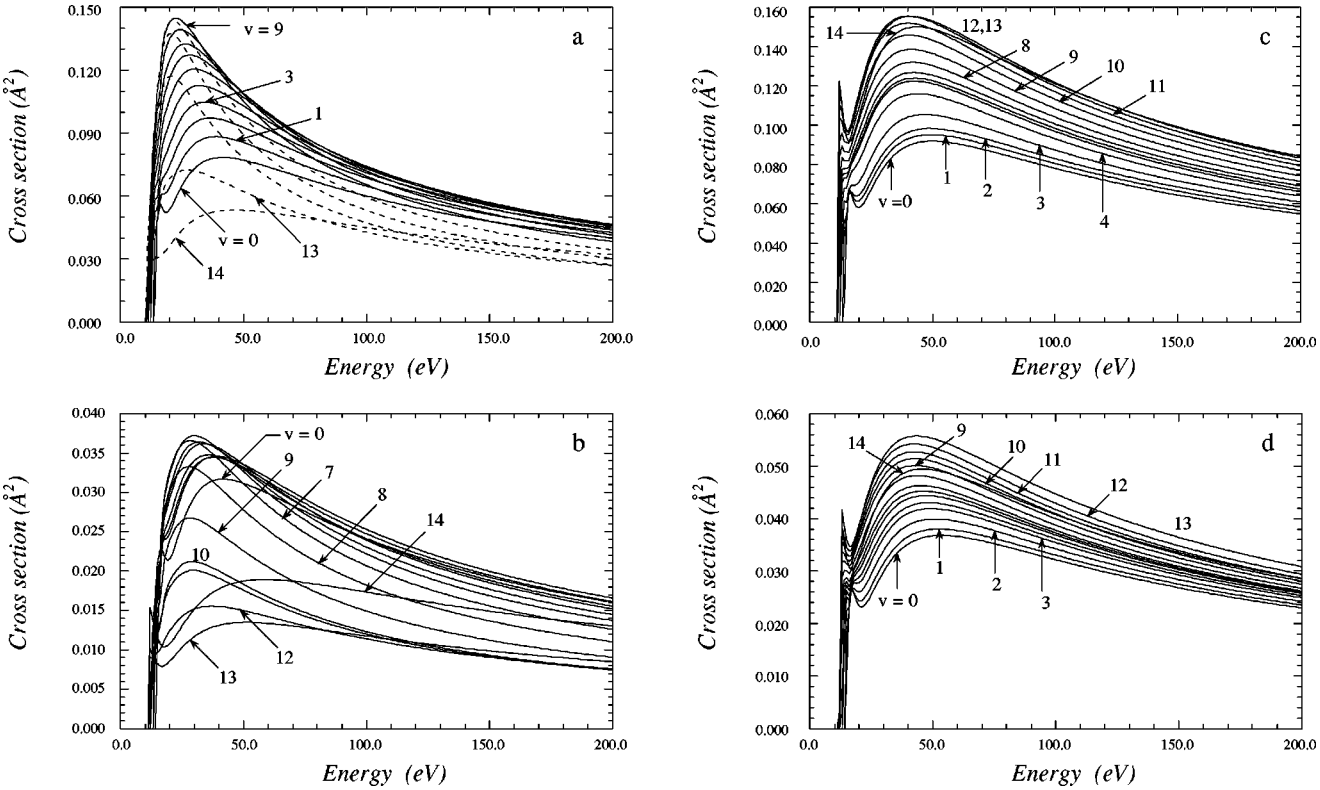

FIG. 1. Total cross sections (bound-bound excitation plus bound-continuum dissociative excitation) as a function of the incident electron energy for the processes: (a) $H_2(X\,^1\Sigma_g^+, \nu_i=0-14)+e\rightarrow H_2(B'\,^1\Sigma_u^+)+e$, (b) $H_2(X\,^1\Sigma_g^+, \nu_i=0-14)+e\rightarrow H_2(B''\,^1\Sigma_u^+)+e$, (c) $H_2(X\,^1\Sigma_g^+, \nu_i=0-14)+e\rightarrow H_2(D\,^1\Pi_u)+e$, (d) $H_2(X\,^1\Sigma_g^+, \nu_i=0-14)+e\rightarrow H_2(D'\,^1\Pi_u)+e$. (a) Solid lines: $\nu_i\leqslant 9$; dashed lines: $\nu_i>9$.

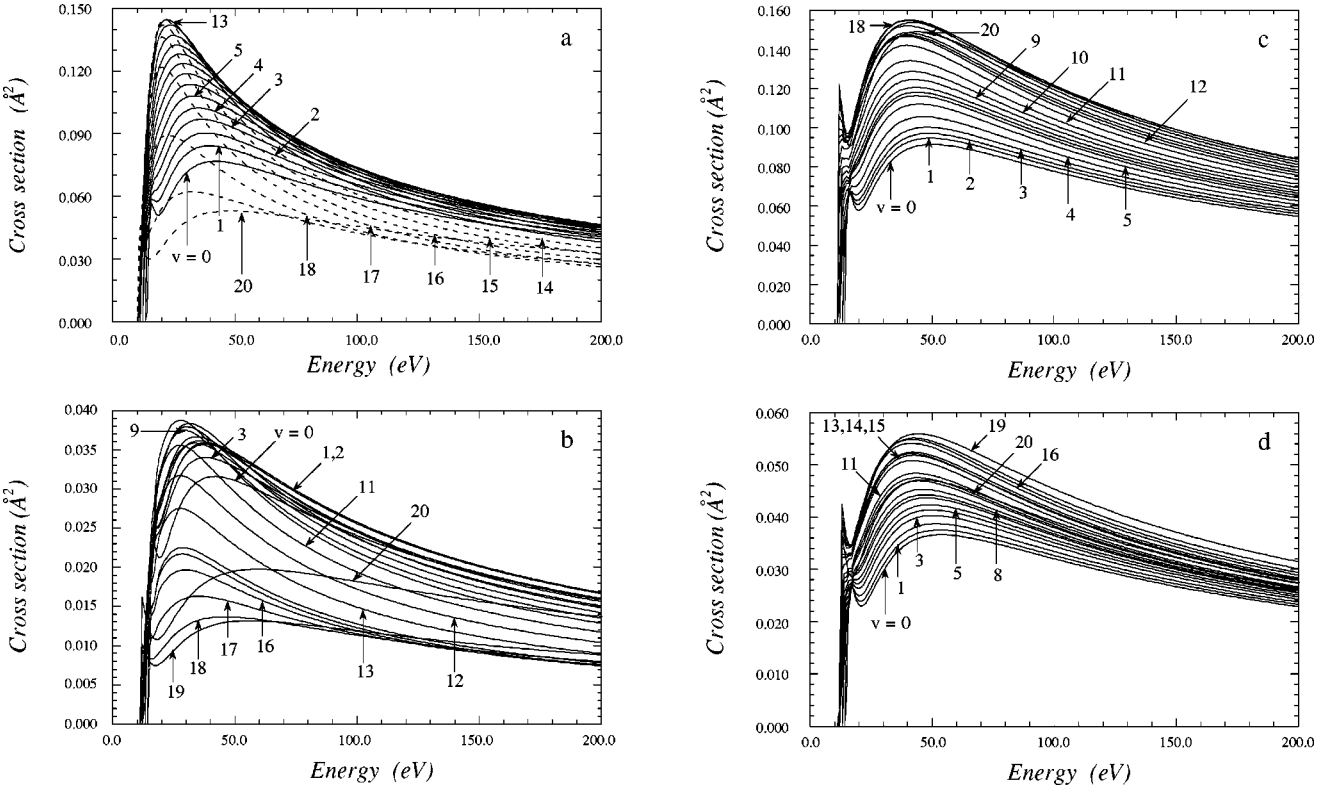

FIG. 2. Same as Fig. 1 for the D_2 molecule with $\nu_i=0-20$. (a) Solid lines: $\nu_i\leqslant 13$; dashed lines: $\nu_i>13$.

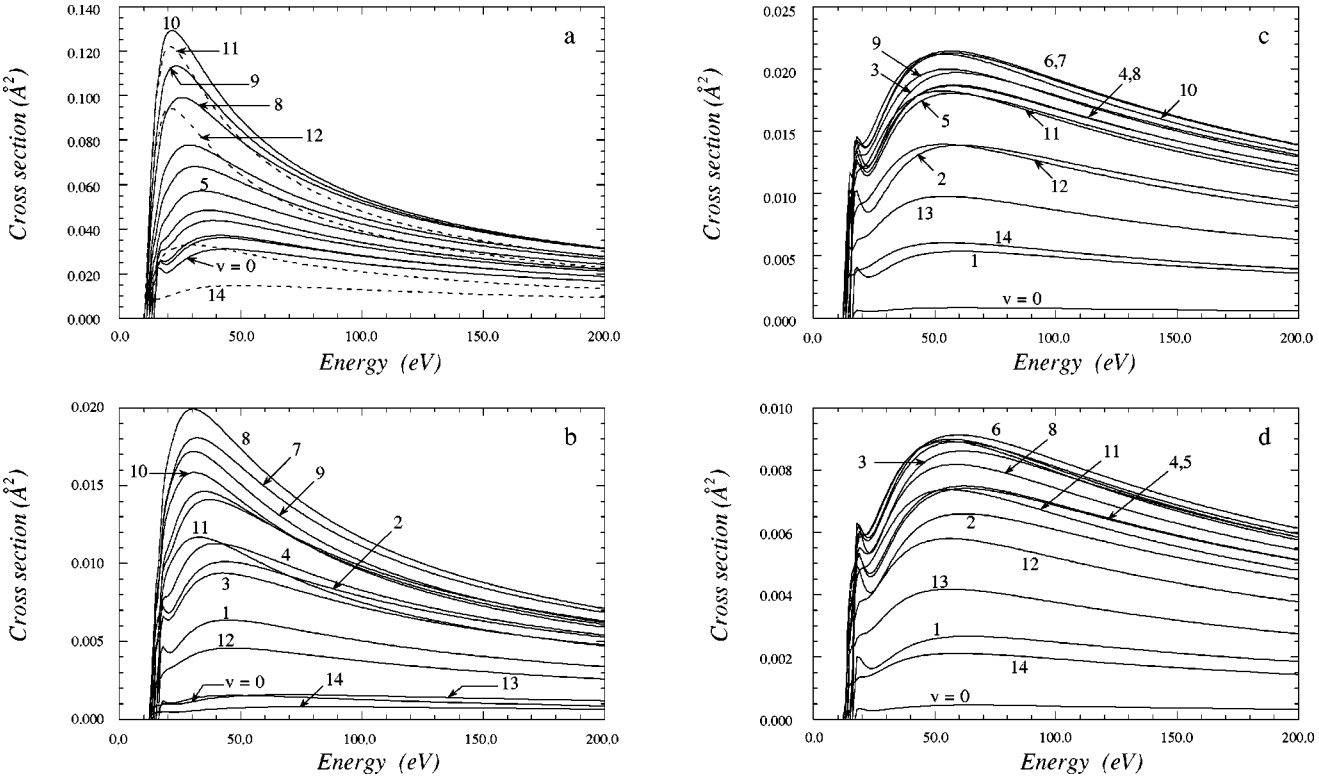

FIG. 3. Same as Fig. 1 for the H_2 dissociative cross sections. (a) Solid lines: $\nu_i \leqslant 10$; dashed lines: $\nu_i > 10$.

$^1\Sigma \rightarrow {}^1\Pi$ transitions the bound-continuum dissociative cross sections present small values compared to the total ones, indicating a large contribution of the bound-bound excitation cross sections. The contrary is true for the $^1\Sigma \rightarrow {}^1\Sigma$ transitions, for which the dissociative cross sections, especially for intermediate values of the vibrational quantum number, turn out to be very high.

A general feature displayed by Fig. 5 is a sort of shift arising in both the total and dissociative cross sections passing from the H_2 to the D_2 molecule. This ''isotopic effect''

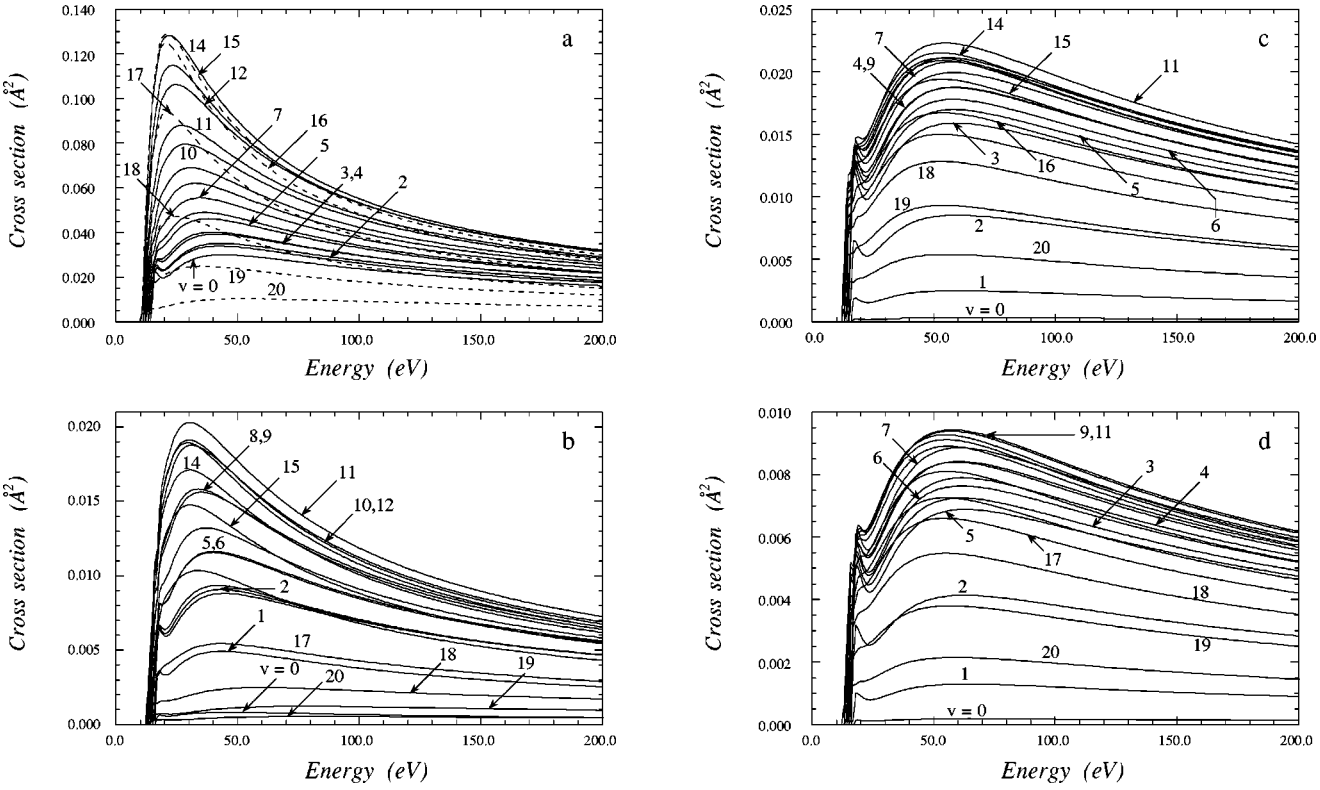

FIG. 4. Same as Fig. 1 for the D_2 dissociative cross sections ($\nu_i = 0$–20). (a) Solid lines: $\nu_i \leqslant 14$; dashed lines: $\nu_i > 14$.

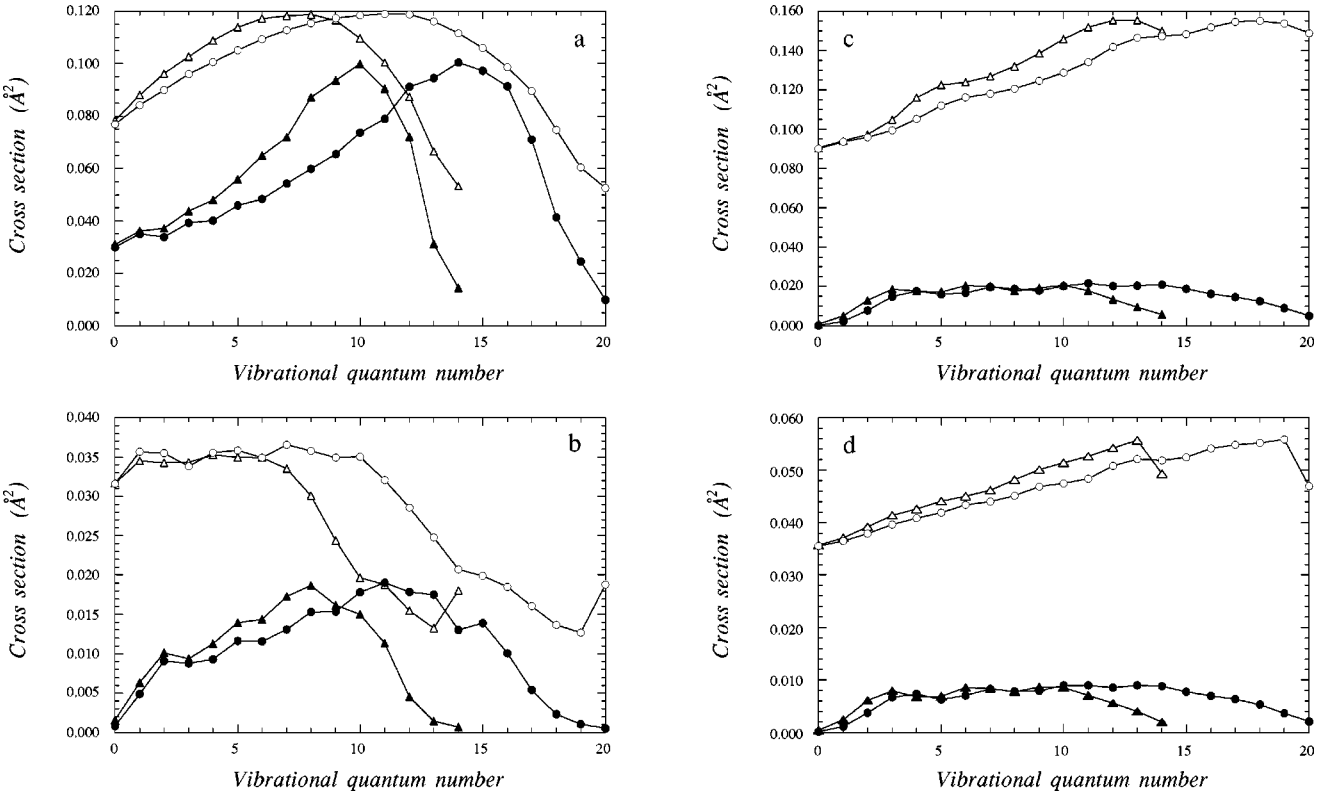

FIG. 5. Total (open circles and triangles) and dissociative (closed circles and triangles) cross sections for H_2 (triangles) and D_2 (circles) molecules as a function of the initial vibrational quantum number and for a fixed incident energy $E = 42$ eV, for the same transitions of Fig. 1.

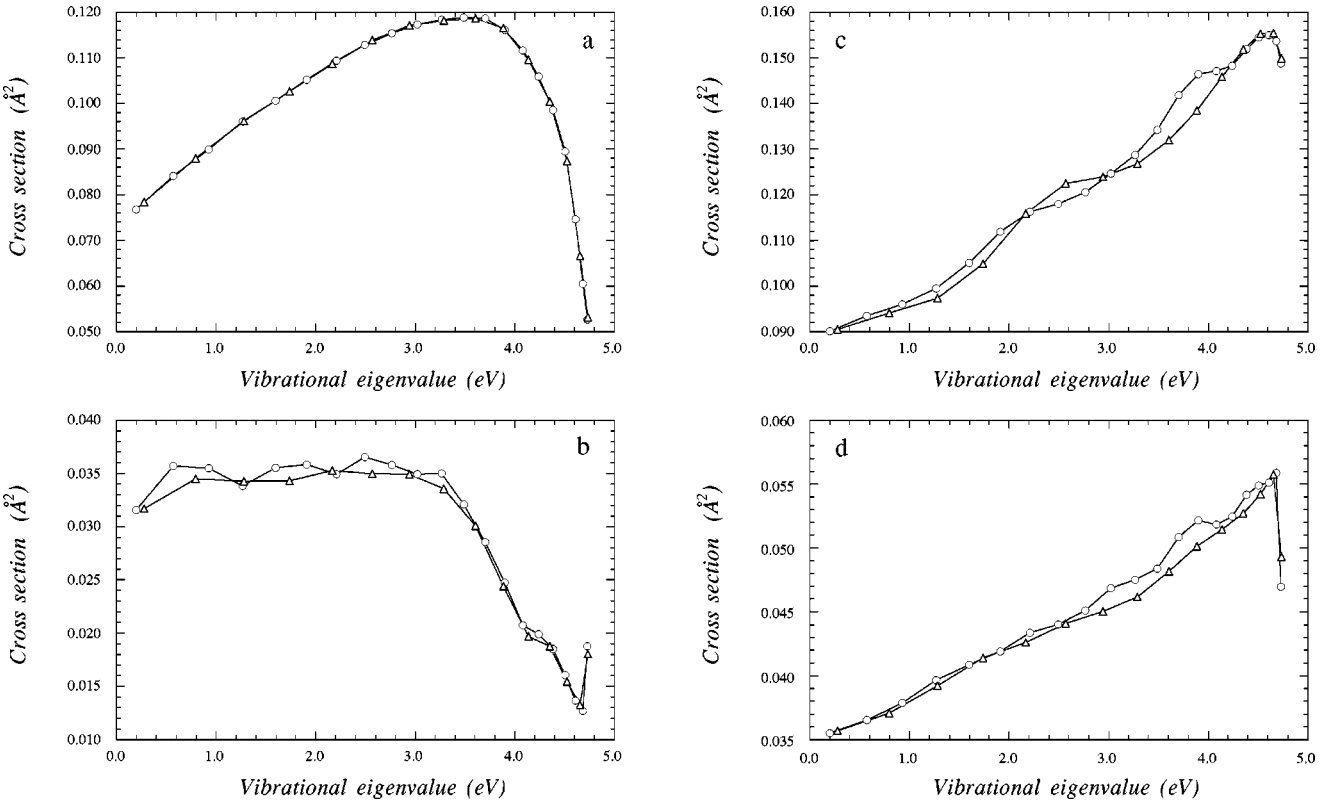

FIG. 6. Total cross sections for H_2 (triangles) and D_2 (circles) molecules as a function of the $X\ ^1\Sigma_g^+$ vibrational eigenvalues and for a fixed incident energy $E = 42$ eV, for the same transitions of Fig. 1.

TABLE III. H_2 and D_2 Born-approximation total cross sections (a_0^2) as a function of the vibrational quantum number and for the incident energies $E=1000$ and 2000 eV.

	$X\rightarrow B'$		$X\rightarrow B''$		$X\rightarrow D$		$X\rightarrow D'$	
ν_{H_2}	1000 eV	2000 eV	1000 eV	2000 eV	1000 eV	2000 eV	1000 eV	2000 eV
0	0.0446	0.0255	0.0176	0.0100	0.0648	0.0375	0.0275	0.0159
1	0.0465	0.0265	0.0180	0.0102	0.0669	0.0387	0.0282	0.0162
2	0.0481	0.0273	0.0173	0.0098	0.0691	0.0399	0.0288	0.0166
3	0.0486	0.0275	0.0165	0.0093	0.0714	0.0412	0.0294	0.0169
4	0.0485	0.0274	0.0159	0.0089	0.0737	0.0425	0.0299	0.0172
5	0.0478	0.0269	0.0149	0.0083	0.0759	0.0438	0.0302	0.0174
6	0.0459	0.0257	0.0138	0.0077	0.0777	0.0448	0.0303	0.0174
7	0.0433	0.0242	0.0125	0.0069	0.0796	0.0459	0.0304	0.0175
8	0.0401	0.0223	0.0108	0.0060	0.0821	0.0473	0.0309	0.0178
9	0.0361	0.0199	0.0089	0.0049	0.0852	0.0490	0.0316	0.0182
10	0.0316	0.0173	0.0075	0.0042	0.0881	0.0507	0.0323	0.0186
11	0.0276	0.0150	0.0075	0.0042	0.0904	0.0521	0.0329	0.0189
12	0.0251	0.0138	0.0083	0.0048	0.0930	0.0536	0.0338	0.0195
13	0.0278	0.0157	0.0104	0.0061	0.0958	0.0552	0.0357	0.0206
14	0.0391	0.0228	0.0168	0.0099	0.0983	0.0569	0.0336	0.0195
ν_{D_2}								
0	0.0443	0.0253	0.0176	0.0100	0.0645	0.0373	0.0274	0.0158
1	0.0456	0.0260	0.0180	0.0102	0.0659	0.0382	0.0279	0.0161
2	0.0470	0.0268	0.0179	0.0102	0.0674	0.0390	0.0283	0.0163
3	0.0481	0.0274	0.0173	0.0098	0.0690	0.0399	0.0288	0.0166
4	0.0485	0.0275	0.0167	0.0094	0.0706	0.0408	0.0292	0.0169
5	0.0486	0.0275	0.0163	0.0092	0.0723	0.0417	0.0296	0.0170
6	0.0485	0.0274	0.0157	0.0088	0.0739	0.0427	0.0299	0.0172
7	0.0480	0.0270	0.0151	0.0085	0.0755	0.0435	0.0301	0.0173
8	0.0469	0.0263	0.0144	0.0080	0.0768	0.0443	0.0302	0.0174
9	0.0454	0.0254	0.0135	0.0075	0.0781	0.0450	0.0303	0.0174
10	0.0436	0.0243	0.0126	0.0070	0.0795	0.0458	0.0304	0.0175
11	0.0414	0.0230	0.0115	0.0064	0.0811	0.0467	0.0307	0.0176
12	0.0388	0.0215	0.0102	0.0056	0.0832	0.0479	0.0312	0.0179
13	0.0358	0.0197	0.0088	0.0049	0.0854	0.0492	0.0317	0.0182
14	0.0327	0.0179	0.0077	0.0043	0.0875	0.0504	0.0322	0.0185
15	0.0297	0.0162	0.0074	0.0042	0.0892	0.0514	0.0326	0.0188
16	0.0268	0.0146	0.0075	0.0042	0.0909	0.0523	0.0330	0.0190
17	0.0252	0.0138	0.0082	0.0047	0.0926	0.0533	0.0336	0.0194
18	0.0257	0.0143	0.0095	0.0055	0.0945	0.0545	0.0347	0.0200
19	0.0304	0.0173	0.0112	0.0066	0.0967	0.0558	0.0367	0.0212
20	0.0403	0.0235	0.0177	0.0105	0.0984	0.0570	0.0324	0.0188

must be considered only apparent, being due to the fact that the cross sections in Fig. 5 are plotted against the vibrational quantum number, while actually they physically depend on the vibrational energy eigenvalues through the transition energy entering in the dynamical factor. In fact, as shown in Figs. 6(a)–6(d), the isotopic effect completely disappears if we report the H_2 and D_2 cross sections as a function of the energy eigenvalues, relative to the ground electronic state vibrational levels, in place of the initial vibrational quantum number.

Born-approximation total cross sections, calculated according to Ref. [22] for both H_2 and D_2 molecules, are reported in Table III as a function of ν_i and for the incident energies of 1000 and 2000 eV. The data relative to 1000 eV have been used to evaluate the $\rho^0_{\nu_i}$ cutoff parameters, as described in the preceding section, and then used to calculate the impact-parameter cross sections for an incident energy of 2000 eV finding a very good agreement with those reported in Table III at the same energy.

Before ending this section, we want to discuss a comparison among our cross sections with different results taken from the literature. The comparison is limited to the $\nu_i=0$ case for which both theoretical and experimental data are available.

Figure 7 shows the dissociative cross sections for the $X\rightarrow B'$ transition from different authors. Our cross sections, together with those from Ref. [26], present at intermediate and high energies lower values with respect to the other cal-

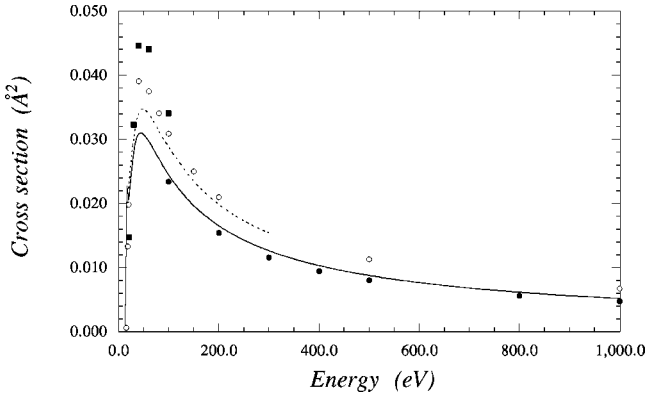

FIG. 7. Dissociative cross sections as a function of incident energy for the process: $H_2(X\,^1\Sigma_g^+, \nu_i=0)+e \rightarrow H_2(B'\,^1\Sigma_u^+)+e \rightarrow H+H+e$. Full line: present results; dashed line: Redmon *et al.* [18] (impact-parameter method); closed circles: Borges *et al.* [26] (Born approximation); squares: Mu-Tao *et al.* [33] (distorted-wave approximation); open circles: Chung *et al.* [32] (modified Born approximation).

culations. The results of Redmon *et al.* [18], who performed their calculation by employing the impact-parameter method used in this work in the same formulation, deserve particular mention. As suggested by Borges *et al.* [26], the discrepancy arising between our results and those of Ref. [18] can be ascribed to the use of different potential curves in evaluating the continuum vibrational wave function. We used the potential energy given by Wolniewicz and Dressler [28], adding two more points at short internuclear distances falling in the region of the repulsive portion of the potential curve (Table II), while Redmon *et al.* employed the experimental *R-K-R* potential reported by Spindler [34]. Actually, a calculation that we performed with the Spindler potential and by using the same cutoff parameter of 1.7 a.u., taken by Redmon *et al.* from the literature and referred to the $X\,^1\Sigma_g^+ \rightarrow B\,^1\Sigma_u^+$ transition, was in very good agreement with their results, reproducing with an average error of 0.9% the cross section values reported for several energies in Table V of their paper. Dissociative cross sections therefore turn out to be somewhat sensitive to the accuracy of the electronic potential. This was confirmed by the fact that assuming for $\rho_{\nu_i}^0$ the more appropriate value for the $X \rightarrow B'$ transition of 1.528 a.u. and using the Spindler potential the recalculated cross sections were in very close agreement with the results of Chung *et al.* [32] (Born approximation and Spindler potential) and Mu-Tao *et al.* [33] (distorted-wave approximation and Spindler potential). For example, at an incident energy of 40 eV, around the maximum, we found a value of 4.01×10^{-18} cm^2 which differs from that of Chung *et al.* (3.91×10^{-18} cm^2) by $\sim$3%, and this difference becomes smaller as the energy increases. Finally, the Born-approximation cross sections, recently calculated by Borges *et al.* [26] using the Wolniewicz and Dressler potential, agree quite well with our results (Fig. 7).

The total cross sections for all the transitions considered here can be compared with the results of Arrighini *et al.* [35] which report the Born-Ochkur total cross sections for several transition processes in the range 20–2000 eV. These calculations show, with respect to impact-parameter results, some difference for the $X \rightarrow B''$ transition, ranging from $\sim$4% at 50 eV to $\sim$14% at 1000 eV. The situation, however, is much better for the other three cases for which, except near the threshold ($<$50 eV) where some deviation is still present, the differences tend to diminish as the energy increases and an excellent agreement is reached at 1000 and 2000 eV with our $\nu=0$ Born-approximation cross sections listed in Table III.

TABLE IV. Scaling law c_i coefficients [Eq. (5.1)].

Coefficient	$X \rightarrow B'$	$X \rightarrow B''$	$X \rightarrow D$	$X \rightarrow D'$
c_1	0.0	0.0	2.93×10^{-3}	1.1×10^{-4}
c_2	0.0	0.0	2.25	3.6
c_3	2.0	-0.2	1.0	0.55
c_4	0.0	0.0	0.20	0.26
c_5	1.1	1.1	1.0	1.0
c_6	-0.13	-0.13	0.0	0.0
c_7	1.94×10^{-2}	1.26×10^{-2}	0.0	0.0
c_8	0.7	0.5	0.0	0.0
c_9	2.42×10^{-2}	3.44×10^{-2}	0.0	0.0
c_{10}	-3.2×10^{-3}	-5.4×10^{-3}	0.0	0.0
c_{11}	-1.08×10^{-4}	-9.20×10^{-5}	0.0	0.0
c_{12}	1.36×10^{-4}	2.55×10^{-4}	0.0	0.0

To our knowledge experimental measurements are scarce and fragmentary [36–40]. Excitation cross section data for several transitions are reported by Ajello *et al.* [38] at 100 eV. The agreement with our results [41] is very good for all the transitions but the $X \rightarrow B'$, for which the experimental excitation cross sections exceed the theoretical ones by more than a factor of 2. This difference, however, is to be considered as a disagreement between theory and experiment, with other theoretical treatments [18,33] in good agreement with our results at the above energy. A similar situation for the dissociative cross sections relative to this last transition has also been found in Ref. [26], to which we refer for an extensive discussion on a discrepant comparison among the calculated cross sections and the measured ones.

The importance of the direct excitation of Rydberg states by electron impact lies in the fact that realistic modeling of hydrogen plasma requires the inclusion of these processes, although they present relatively low excitation cross sections. Actually, a comparison with the $\nu_i=0$ cross sections for the $X \rightarrow B(^1\Sigma_u^+, 2p\sigma)$ and $X \rightarrow C(^1\Pi_u, 2p\pi)H_2$ transitions, calculated by Celiberto and Rescigno [20] by using a modified form of the impact-parameter method, shows in effect that they are about a factor of 10 or more higher than the present results. On the other hand, collisional-radiative models can be satisfactorily built up only if complete sets of cross sections for processes leading to the whole electronic and vibrational manifold are available.

To understand this point, it is sufficient to point out that, as proposed in a recent paper of Pinnaduwage *et al.* [42], the cross sections for dissociative attachment to Rydberg H_2 molecules [process (1.1)], as well as the corresponding rates, can be simply scaled as $n^{7/2}$. Such a scaling indicates the importance of the very highly excited electronic states in the global attachment process [9], despite the n^{-3} dependence shown by their electron-collision excitation cross sections and rates [6,15]. At the same time, it is known that the direct

TABLE V. Fitting coefficients a_i and transition energies ΔE_{ν_i} for the $\nu_i=0,1$ H_2 cross sections [Eq. (5.3)].

	$X\to B'$		$X\to B''$		$X\to D$		$X\to D'$	
	$\nu_i=0$	$\nu_i=1$	$\nu_i=0$	$\nu_i=1$	$\nu_i=0$	$\nu_i=1$	$\nu_i=0$	$\nu_i=1$
a_1 (Å^2)	−0.0828	−0.114	−0.0399	−0.0507	0.586	0.529	0.278	0.288
a_2	0.387	0.371	0.456	0.419	1.678	1.238	1.867	1.544
a_3 (Å^2)	0.187	0.215	0.0694	0.0776	0.310	0.361	0.127	0.145
a_4	1.334	1.352	1.494	1.514	0.794	0.698	0.781	0.703
ΔE_{ν_i} (eV)	14.85	13.09	15.67	13.86	14.99	13.35	15.66	14.04

ionization from high Rydberg states plays a crucial role in the global ionization process of molecular hydrogen [14].

V. SCALING RELATIONS

Due to the importance of electron-molecule cross sections in many fields of molecular physics, we give here some analytical expressions able to reproduce the present data for practical applications.

A scaling relationship for H_2 total cross sections, in terms of the vibrational quantum number ν_i, can be written as

$$\sigma_\nu(x)=\sigma_{\nu=1}(x)\left[\frac{\Delta E_{\nu=1}}{\Delta E_\nu}\right]^{(1+c_1\nu^{c_2})[c_3+(2/x)^{c_4}]} \times\left\{c_5+c_6\nu+\left(\frac{c_7}{x^{c_8}}+c_9\right)\nu^2+c_{10}\nu^3 +\left(\frac{c_{11}}{x^{c_8}}+c_{12}\right)\nu^4\right\}, \tag{5.1}$$

where the reduced energy is defined as $x=E/\Delta E_{\nu_i}$ and ΔE_{ν_i} is the total vertical transition energy expressed as the difference between the potential energies involved in the transition, evaluated at the largest classical turning point R_{ν_i} of the ν_ith vibrational level of the ground electronic state, i.e. [43,44],

$$\Delta E_{\nu_i}=V_{\text{excited}}(R_{\nu_i})-V_{\text{ground}}(R_{\nu_i}). \tag{5.2}$$

The c_i coefficients are given in Table IV. Equation (5.1) represents the total cross section $\sigma_{\nu_i}^{X\to\alpha}(x)$ for each $\nu_i>1$ vibrational level in terms of the $\nu_i=1$ total cross section $\sigma_{\nu_i=1}^{X\to\alpha}(x)$. This last quantity, together with the $\nu_i=0$ cross sections, can be obtained by using the following fitting expression:

$$\sigma_{\nu_i}^{X\to\alpha}(x)=\frac{1}{x}[a_1\exp(-a_2x)+a_3\ln(a_4x)]. \tag{5.3}$$

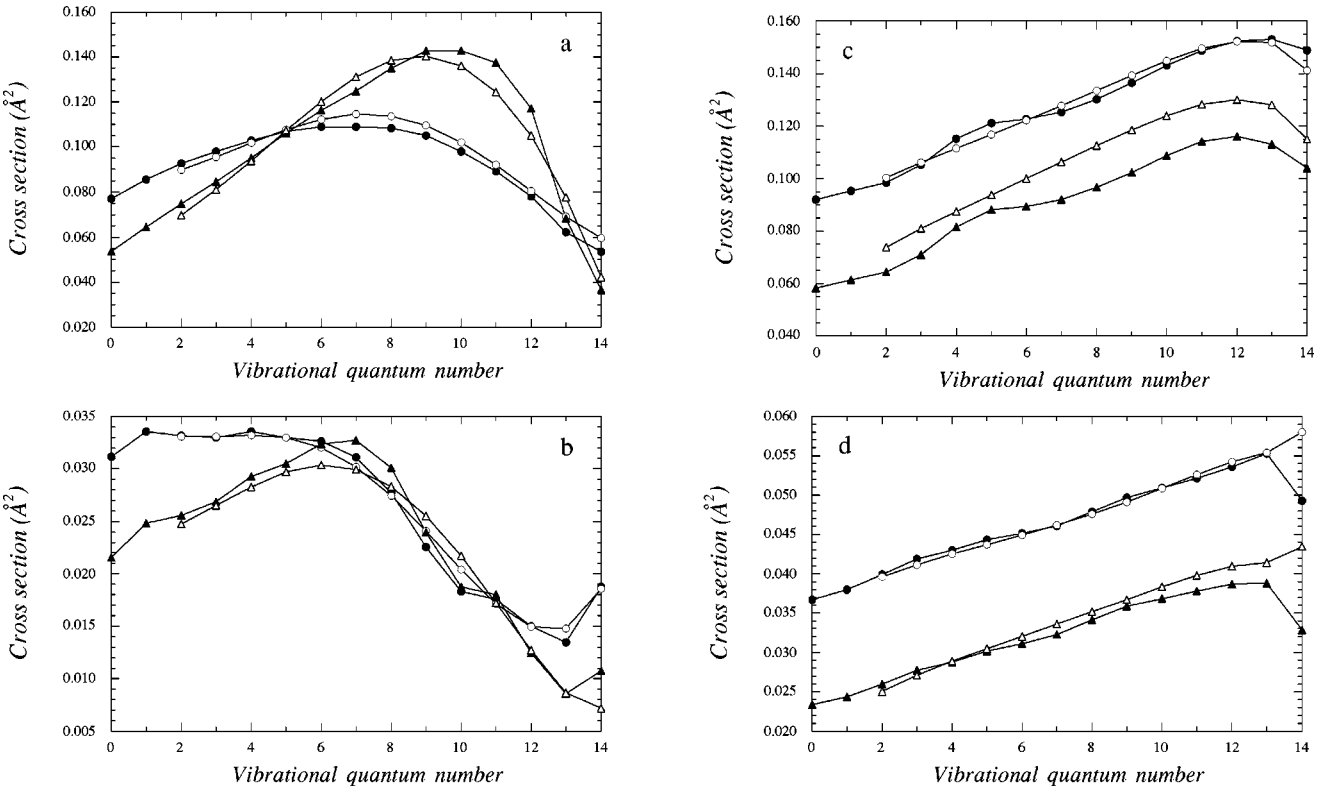

FIG. 8. Comparison between the scaled (open circles and triangles) and impact-parameter (closed circles and triangles) cross sections at two different energies $E=20$ eV (triangles) and $E=50$ eV (circles) for the same transitions of Fig. 1.

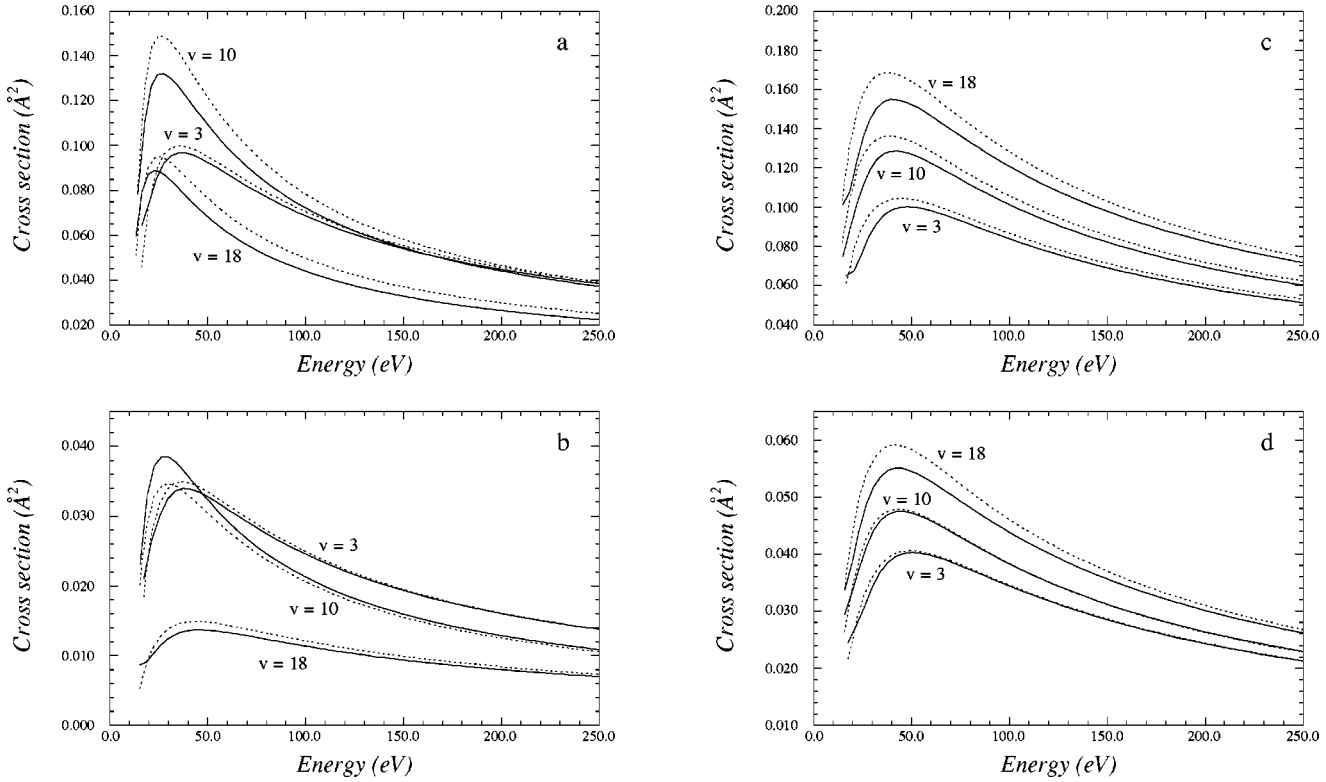

FIG. 9. Comparison between the scaled (dotted lines) and impact-parameter (full lines) cross sections for D_2 molecules for $\nu_i = 3,10,18$ for the same transitions of Fig. 1.

The a_i coefficients for $\nu_i = 0,1$ and relative transition energies, entering in the definition of x, are reported in Table V.

Figures 8(a)–8(d) show the total cross sections for the four transitions as a function of the vibrational quantum number for two incident energies of 20 and 50 eV. A satisfactory agreement is found in all the cases except for the $X \rightarrow D$ transition, where some discrepancy arises near the threshold (20 eV) not exceeding, however, a factor of $\sim 15\%$. Large differences are found for $\nu_i = 14$ for the two $X \rightarrow D'$ and $X \rightarrow B''$ transitions. Expression (5.3) can also be used for very high energies. The scaled cross sections for 1000 eV, in fact, show the same accuracy observed in Fig. 8. However, a more physical expression can be used in the $E \rightarrow \infty$ asymptotic region. In this case, in fact, Eq. (2.1) can be put in the form (a.u.) [18–20]

$$\sigma_{\nu_i}^{X \rightarrow \alpha}(E) = \text{const} \times \langle \nu_i | M^2(R) | \nu_i \rangle \frac{1}{E} \ln\left(\frac{\rho_{\nu_i}^0 \Delta E_{\nu_i}}{\sqrt{2E}} \right). \tag{5.4}$$

Once again ΔE_{ν_i} is the vertical transition energy and $\rho_{\nu_i}^0$ the cutoff parameter. The dipole moment matrix elements $\langle \nu_i | M^2(R) | \nu_i \rangle$, as well as the quantity $\rho_{\nu_i}^0 \Delta E_{\nu_i}$, can be simultaneously obtained for each ν_i level by using the Born cross sections reported in Table III at incident energies of 1000 and 2000 eV. Expression (5.4) can be confidently used for 300 eV upward. The discrepancies with the ''exact'' cross sections are very small at 300 eV and practically vanish as the energy increases.

The deuterium cross sections can be obtained by using the corresponding ones for H_2. A mass scaling law, in fact, can be established by exploiting the ''isotopic effect'' discussed in the preceding section. We have, in fact, seen that the H_2 and D_2 cross sections are practically invariant once expressed in terms of the same vibrational energy eigenvalue. A scaling law can therefore be derived by assuming a correspondence between deuterium and hydrogen eigenvalues, i.e.,

$$E_{\nu_i}^{D_2} \approx E_{\nu'}^{H_2}. \tag{5.5}$$

Expressing the energies in the harmonic oscillator approximation ($E_\nu \approx \hbar \omega \nu$) we get

$$\nu' \approx \frac{\omega_{D_2}}{\omega_{H_2}} \nu_i. \tag{5.6}$$

From this relation we may obtain the (noninteger) vibrational quantum number ν' corresponding to the hydrogen $\sigma_{\nu'}^{X \rightarrow \alpha}(x)$ cross section which can be calculated by inserting ν' in Eq. (5.1), beside the vertical transition energy evaluated at the largest classical turning point of the deuterium ν_i level.

Equation (5.6) can be further simplified. The mass scaling factor in fact, can be explicitly obtained by expressing the oscillator frequencies in Eq. (5.6) in terms of the reduced mass of the molecules, i.e.,

$$\nu' = \sqrt{\frac{\mu_{H_2}}{\mu_{D_2}}} \nu_i. \tag{5.7}$$

By recalling that $\mu_{D_2} \approx 2\mu_{H_2}$, we get the final result

$$\nu' \approx \frac{1}{\sqrt{2}}\nu_i . \tag{5.8}$$

This simple relation has been found to be extremely powerful. Actually, inspection of Figs. 9(a)–9(d) shows a very satisfactory agreement between the impact-parameter total cross sections for the D_2 molecule, plotted as a function of the incident energy for $\nu_i = 3,10,18$, with the scaled ones obtained by using Eqs. (5.8) and (5.1). The differences observed around the maximum are mainly due to the error inherent in the vibrational scaling expression adopted for reproducing H_2 cross sections. Equation (5.8) is to be used for $\nu_i > 1$ since the deuterium and hydrogen cross sections for $\nu_i = 0,1$ are practically the same. The validity of relations, analogous to Eqs. (5.6) and (5.7), has been verified for other hydrogen isotopes as well [45].

VI. CONCLUSIONS

In this paper we have presented electron-molecule cross sections for excitation and dissociative excitation of vibrationally excited H_2 and D_2 molecules to electronic Rydberg states ($X\,^1\Sigma_g^+ \rightarrow B'\,^1\Sigma_u^+$, $B''\,^1\Sigma_u^+$, $D\,^1\Pi_u$, $D'\,^1\Pi_u$). The present results, obtained by using the quantum mechanical impact-parameter method, represent a complete set of cross sections for the excitation to the first Rydberg states as a function of the vibrational levels and covering a wide range of incident energies ranging from the threshold to thousands of eV. Due to the growing interest in the role that the electronically excited states can play in many hydrogen plasmas [46] and to the related needs of reliable cross section data [47], we provided some simple scaling relations and analytical expressions which permit a rapid evaluation of the total cross sections in terms of both the initial vibrational quantum number and energy. These expressions can also be extended beyond the range of incident energies considered here.

ACKNOWLEDGMENTS

This work has been partially supported by MURST (under Project No. 9703109065006) and by CNR (short-term mobility program).

[1] M. Capitelli, M. Cacciatore, R. Celiberto, F. Esposito, C. Gorse, and A. Laricchiuta, Plasma Phys. Rep. **25**, 3 (1999), and references quoted herein.
[2] M. Capitelli, R. Celiberto, and M. Cacciatore, in *Advances in Atomic, Molecular and Optical Physics*, edited by M. Inokuti (Academic Press, New York, (1994), Vol. 33, p. 321.
[3] J.M. Wadehra and J.N. Bardsley, Phys. Rev. Lett. **41**, 1795 (1978); Phys. Rev. A **20**, 1398 (1979); J.M. Wadehra *ibid.* **29**, 106 (1984); D.E. Atems and J.M. Wadehra, J. Phys. B **26**, L759 (1993). See also J.M. Wadehra, in *Nonequilibrium Vibrational Kinetics*, edited by M. Capitelli, Topics in Current Physics Vol. 39 (Springer-Verlag, Berlin, 1986), p. 191.
[4] L.A. Pinnaduwage and L.G. Christophorou, Phys. Rev. Lett. **70**, 754 (1993); J. Appl. Phys. **76**, 46 (1994).
[5] P.G. Datdkos, L.A. Pinnaduwage, and J.F. Kielkopf, Phys. Rev. A **55**, 4131 (1997).
[6] J.R. Hiskes, Appl. Phys. Lett. **69**, 755 (1996); in *Production and Neutralization of Negative Ions and Beams*: *Seventh International Symposium/Production and Application of Light Negative Ions: Sixth European Workshop*, edited by K. Prelec, AIP Conf. Proc. 380 (AIP, New York, 1996), p. 61.
[7] C. Gorse, M. Capitelli, R. Celiberto, D. Iasillo, and S. Longo, in *Production and Neutralization of Negative Ions and Beams*: *Seventh International Symposium/Production and Application of Light Negative Ions: Sixth European Workshop* (Ref. [6]), p. 109.
[8] A. Garscadden and R. Nagpal, Plasma Sources Sci. Technol. **4**, 268 (1995).
[9] K. Hassouni, A. Gicquel, and M. Capitelli, Chem. Phys. Lett. **290**, 502 (1998).
[10] R.K. Janev, in *Atomic and Molecular Processes in Fusion Edge Plasmas*, edited by R.K. Janev (Plenum Press, New York, 1995), p. 1.
[11] T. Fujimoto, K. Sawada, and K. Takahata, J. Appl. Phys. **66**, 2315 (1989).
[12] T. Fujimoto and R.W.P. McWhirter, Phys. Rev. A **42**, 6588 (1990).
[13] K. Sawada, K. Eriguchi, and T. Fujimoto, J. Appl. Phys. **73**, 8122 (1993).
[14] K. Sawada and T. Fujimoto, Phys. Rev. E **49**, 5565 (1994); J. Appl. Phys. **78**, 2913 (1995).
[15] J.A. Schiavone, S.M. Tarr, and R.S. Freund, J. Chem. Phys. **70**, 4468 (1979).
[16] T.E. Sharp, At. Data **2**, 119 (1971).
[17] A.U. Hazi, Phys. Rev. A **23**, 2232 (1981).
[18] M.J. Redmon, B.C. Garrett, L.T. Redmon, and C.W. McCurdy, Phys. Rev. A **32**, 3354 (1985).
[19] B.C. Garrett, L.T. Redmon, C.W. McCurdy, and M.J. Redmon, Phys. Rev. A **32**, 3366 (1985).
[20] R. Celiberto and T.N. Rescigno, Phys. Rev. A **47**, 1939 (1993).
[21] R. Celiberto, U.T. Lamanna, and M. Capitelli, Phys. Rev. A **50**, 4778 (1994).
[22] R. Celiberto, M. Capitelli, N. Durante, and U.T. Lamanna, Phys. Rev. A **54**, 432 (1996).
[23] R. Celiberto, U.T. Lamanna, and M. Capitelli, Phys. Rev. A **58**, 2106 (1998).
[24] S.E. Branchett and J. Tennyson, J. Phys. B **25**, 2017 (1992).
[25] A.L. Ford, J.C. Browne, E.J. Shipsey, and P. DeVries, J. Chem. Phys. **63**, 362 (1975).
[26] I. Borges, Jr., G. Jalbert, and C.E. Bielschowsky, Phys. Rev. A **57**, 1025 (1998).
[27] $X\,^1\Sigma_g^+$ state: W. Kolos and L. Wolniewicz, J. Chem. Phys. **43**, 2429 (1965).
[28] $B'\,^1\Sigma_u^+$ and $D\,^1\Pi_u$ state: L. Wolniewicz and K. Dressler, J. Chem. Phys. **88**, 3861 (1988).
[29] $B''\,^1\Sigma_u^+$ state: W. Kolos, J. Mol. Spectrosc. **62**, 429 (1976).
[30] F.L. Tobin and J. Hinze, J. Chem. Phys. **63**, 1034 (1975).
[31] S. Geltman, *Topics in Atomic Collision Theory* (Academic Press, New York, 1969).

[32] S. Chung, C.C. Lin, and E.T.P. Lee, Phys. Rev. A **12**, 1340 (1975).
[33] L. Mu-Tao, R.R. Lucchese, and V. McKoy, Phys. Rev. A **26**, 3240 (1982).
[34] R.J. Spindler, Jr., J. Quant. Spectrosc. Radiat. Transf. **9**, 1041 (1969).
[35] G.P. Arrighini, F. Biondi, and C. Guidotti, Mol. Phys. **41**, 1501 (1980).
[36] J.M. Ajello, D. Shemansky, T.L. Kwok, and Y.L. Yung, Phys. Rev. A **29**, 636 (1984).
[37] D.E. Shemansky, J.M. Ajello, and D.T. Hall, Astrophys. J. **296**, 765 (1985).
[38] J.M. Ajello, D.E. Shemansky, B. Franklin, J. Watkins, S. Srivastava, G.K. James, W.T. Simms, C.W. Hord, W. Pryor, W. McClintock, V. Argabright, and D. Hall, Appl. Opt. **27**, 890 (1988).
[39] J.M. Ajello, D.E. Shemansky, and G.K. James, Astrophys. J. **371**, 422 (1991).
[40] W.T. Miles, R. Thompson, and A.E.S. Green, J. Appl. Phys. **43**, 678 (1972).
[41] Experimental excitation cross section values at 100 eV from Ref. [38]: $B'\,^1\Sigma_u^+$ (0.082 Å^2), $B''\,^1\Sigma_u^+$(0.025 Å^2), $D\,^1\Pi_u$ (0.067 Å^2), $D'\,^1\Pi_u$(0.034 Å^2); present theoretical values: $B'\,^1\Sigma_u^+$(0.036 Å^2),$B''\,^1\Sigma_u^+$ (0.023 Å^2), $D\,^1\Pi_u$ (0.077 Å^2), and $D'\,^1\Pi_u$ (0.032 Å^2).
[42] L.A. Pinnaduwage, W.X. Ding, D. L. McCorkle, S.H. Lin, A.M. Mebel, and A. Garscadden, J. Appl. Phys. **85**, 7064 (1999).
[43] R. Celiberto, M. Capitelli, and R.K. Janev, Chem. Phys. Lett. **256**, 575 (1996).
[44] R. Celiberto, M. Capitelli, and R.K. Janev, Chem. Phys. Lett. **278**, 154 (1997).
[45] R. Celiberto and R.K. Janev (unpublished).
[46] C.S. Sartori, F.J. da Paixão, and M.A.P. Lima, Phys. Rev. A **58**, 2857 (1998).
[47] R. Celiberto and R.K. Janev, IAEA, International Nuclear Data Committee Report No. INDC(NDS)-333, 1995; R. Celiberto, A. Laricchiuta, M. Capitelli, R.K. Janev, J. Wadehra, and D. E. Atems, International Atomic Energy Agency report (unpublished).